JOURNAL OF CATALYSIS **127**, 489–511 (1991)

CO Oxidation over Pd and Cu Catalysts

II. Unreduced Bimetallic $PdCl_2$–$CuCl_2$ Dispersed on Al_2O_3 or Carbon

KYUNG I. CHOI AND M. ALBERT VANNICE

Department of Chemical Engineering, The Pennsylvania State University,
University Park, Pennsylvania 16802

Received May 9, 1990; revised August 27, 1990

Specific activities for CO oxidation by molecular oxygen over unreduced $PdCl_2$–$CuCl_2$ catalysts are higher than on the reduced bimetallic catalysts. This activity is further enhanced by 1–3 orders of magnitude by addition of H_2O vapor to the feed, thus producing very active catalysts at 300 K. The role of the water is twofold: it dissolves the Pd and Cu precursor compounds in a very thin, two-dimensional aqueous layer on the support surface and it also reacts directly with PdClCO, which was identified by IR spectroscopy. Based on this picture, the use of a higher surface area, more hydrophobic carbon support gave the most active catalyst of all. Based on the species detected by IR spectroscopy and their interactions with the reactants as well as a complete kinetic study coupled with recent results reported in the literature, reaction models applicable to the presence and absence of H_2O vapor are proposed. Both O_2 and H_2O are oxidants in the former sequence whereas only molecular oxygen is involved in the catalytic cycle in the latter situation. The principal role of Cu is the reoxidation of $Pd^{(0)}$ when H_2O vapor is present, as in the Wacker process, whereas it appears to be involved as a reactive intermediate also containing Pd, CO, and O_2 in the absence of H_2O vapor.

INTRODUCTION

CO oxidation over unreduced $PdCl_2$–$CuCl_2$ catalysts, which are used in the Wacker process to produce acetaldehyde from ethylene and dioxygen, has attracted attention because of the much higher activity that occurs at low temperature compared to either unreduced or reduced monometallic catalysts (*1–7*). The activity is high enough at 300 K that catalysts containing these metal salts are used commercially to remove CO from room air (*8*). Even though much is known about the reaction mechanism in the Wacker process (*9, 10*), the reaction mechanism for CO oxidation in the presence of these two metal salts is not established, and several reaction mechanisms have been proposed, each of which predicts a different kinetic rate expression. Desai *et al.* (*1, 2*) have proposed a reaction mechanism in which the partial pressure dependency on CO is unity and that on O_2 is minus one-half. With the mechanism of Golodov *et al.* (*3–7*), the partial pressure dependency of the rate on CO is again unity, however, the rate is independent of O_2 partial pressure. As in the Wacker process, both studies proposed that the role of $CuCl_2$ was to reoxidize the Pd metal which had been formed during the production of CO_2. Zhizhina and co-workers (*11–14*) studied a series of oxidants other than $CuCl_2$, and they also concluded that these oxidants played a role in regenerating an oxidized Pd species, which had been reduced initially by the presence of CO and H_2O. However, they proposed that a Pd(I) species, $[Pd_2(CO)]^{+2}$, was the catalytically active species, which differed from the proposals of Desai *et al.* and Golodov *et al.* that Pd(II) species were responsible for CO_2 formation, yet they observed the same partial pressure dependencies on CO and O_2 as Golodov *et al.* All of these previous studies

0021-9517/91 $3.00

TABLE 1

Catalytic Activities and Apparent Activation Energies for CO Oxidation over Unreduced $PdCl_2$–$CuCl_2$ Catalysts with No Pretreatment

Catalyst	P_{H_2O} (Torr)	E_{app}[a] (kcal/mole)	Activity[b] at 300 K (μmole CO/g · s × 10^3)	TOF[b,c] at 300 K ($s^{-1} \times 10^3$)
1.8% Pd–11.9% Cu/δ-Al_2O_3 (Run 1)	0	10.4 ± 2.6	93.4	0.55
(IR)	5.3	16.4 ± 2.5	698	4.3
1.8% Pd–11.9% Cu/δ-Al_2O_3	0	10.9 ± 0.2	11.6	0.069
(reactor)	5.3	9.9 ± 1.5	215	1.27
1.8% Pd–11.8% Cu/carbon (Run 2)	0	10.6 ± 0.05	1.3	0.008
(reactor)	5.3	−5.8 ± 0.8	3411	20.7
0.2% Pd–11.5% Cu/carbon (reactor)	5.3	−7.1 ± 0.2	446	22.6

[a] Uncertainty is represented by 95% confidence limits.

[b] Standard reaction conditions: P_{O_2} = 132 Torr, P_{CO} = 26 Torr, total P = 750 Torr, based on dry wt.

[c] TOF = molecule CO reacted per second per Pd atom.

have shown unequivocally that water plays an important role in CO oxidation over these unreduced Pd–Cu catalysts.

This study was conducted to:

(1) determine the kinetic behavior of CO oxidation over unreduced $PdCl_2$–$CuCl_2$ catalysts utilizing either Al_2O_3 or carbon as a support;

(2) apply IR spectroscopy to see what carbonyl species exist prior to and during reaction conditions;

(3) clarify the role of water by using both hydrophilic and hydrophobic supports;

(4) determine if a reaction sequence could be proposed that was consistent with these results. Surprisingly, no IR studies of CO interacting with these unreduced catalysts had been reported, and this additional information could provide significant new insight into the surface chemistry that occurs.

EXPERIMENTAL

The Pd–Cu catalysts were prepared by simultaneously impregnating the support with both metals using an incipient wetness method (*15*). The supports and the metal precursors of these bimetallic catalysts are identical to those used to prepare the Pd-only or Cu-only catalysts in the previous paper (*16*). The supports were δ-Al_2O_3 (W. R. Grace, 138 m^2/g) and carbon black (Black Pearls 2000, Carbot Corp., 1400 m^2/g), and the metal precursors were $PdCl_2$ (Alfa Products) and $CuCl_2$ (99.999%, Aldrich Chemical Co.). In addition, $Cu(NO_3)_2 \cdot 5H_2O$ (99.999%, Aldrich Chemical Co.), was used to prepare a catalyst containing much less chloride. Sample preparation, equipment, and data acquisition methods are the same as those described in the first paper in this series (*16*).

RESULTS

Kinetic Results

The kinetic parameters of supported, unreduced $PdCl_2$–$CuCl_2$ catalysts in the presence and absence of H_2O vapor are given in Tables 1 and 2, the changes in kinetic parameters due to treatment are given in Table 3; and representative Arrhenius plots for these catalysts are shown in Figs. 1 to 4. Activities are given on a dry weight basis after drying at 573 K. Specific activities are given in the form of a nominal TOF, which is normalized to the Pd atoms in the catalyst assuming the dispersion of the Pd precursor is unity, because Cu by itself has extremely low activity (*16*). Partial pressure dependen-

TABLE 2

Partial Pressure Dependencies on CO, O_2, and H_2O for CO Oxidation over Unreduced $PdCl_2$–CuCl Catalysts with No Pretreatment

Catalyst	Partial pressure dependency[a]			Partial pressure run temp. (K)
	X	Y	Z	
1.8% Pd–11.9% Cu/δ-Al_2O_3 (IR)	0.7 ($P_{CO} < 26$ Torr) 0.1 ($P_{CO} > 26$ Torr)	0.6	No H_2O	353
1.8% Pd–11.8% Cu/carbon (reactor)	0.5 ($P_{CO} < 26$ Torr) 0.1 ($P_{CO} > 26$ Torr)	1.1	No H_2O	363
1.8% Pd–11.9% Cu/δ-Al_2O_3	−0.6	1.1	1.1	303
(IR)	−0.6	0.9	0.1	323
1.8% Pd–11.9% Cu/δ-Al_2O_3	−0.6 ($P_{CO} > 5$ Torr)	1.1	1.1	303
(reactor)	−0.6 ($P_{CO} > 13$ Torr) 0.7 ($P_{CO} < 13$ Torr)	1.2	0.5	323
1.8% Pd–8% Cu/carbon	0.8	0.6	0.9	303
			0.9	323
0.2% Pd–11.5% Cu/carbon	—	—	1.2	303
			1.5	323
2% Pd–11.8% Cu/carbon[b]	0.3	0	2.5	303

[a] $r = kP_{CO}^{X}P_{O_2}^{Y}P_{H_2O}^{Z}$.
P_{CO} = 26 Torr when Y and Z were obtained.
P_{O_2} = 132 Torr when X and Z were obtained.
P_{H_2O} = 5.3 Torr when X and Y were obtained.

[b] Prepared from $PdCl_2$ and $Cu(NO_3)_2 \cdot 5H_2O$.

cies were determined and initially fitted by a power rate law over certain pressure regimes, which varied from 1 to 26 Torr for CO, from 26 to 184 Torr for O_2, and from 2 to 20 Torr for H_2O, and the data are shown in Fig. 5.

For the 1.8% Pd–11.9% Cu/δ-Al_2O_3 catalyst at 353 K with no water vapor in the feed, the CO partial pressure dependency was close to 0.7 when P_{CO} was below 26 Torr but approached zero at higher pressures, while the dependency on O_2 was positive and equal to 0.6, as shown in Fig. 5a. The initial activation energy was 10.4 kcal/mole from the IR reactor results and 10.9 kcal/mole from the kinetic study using the microreactor. After the partial pressure dependency runs for CO and O_2 in the IR reactor were completed, the activation energy was remeasured, as shown in Fig. 1a, and it changed little (11.2 kcal/mol). However, after drying in flowing He at 573 K for 1 h the activation energy had increased to 17 kcal/mole and the room temperature (RT) activity showed a 60-fold decline (Fig. 1b). A subsequent calcination at 573 K in flowing O_2 for an hour did not alter the RT activity noticeably but it reduced the activation energy to 14.9 kcal/mole, as shown in Fig. 1b, and it decreased the O_2 pressure dependency to 0.1 while the CO dependency remained at 0.7.

All studies on the carbon-supported catalysts were conducted in the microreactor because no dispersive IR data could be obtained. The 1.8% Pd–11.9% Cu/carbon catalyst at 363 K without water vapor in the feed gave a CO partial pressure dependency of 0.5 below 26 Torr while it was near zero above 26 Torr, as shown in Fig. 5b. These results were essentially identical to those obtained for the δ-Al_2O_3-supported catalyst; however, the partial pressure dependency on O_2 was 1.1, which is slightly higher than

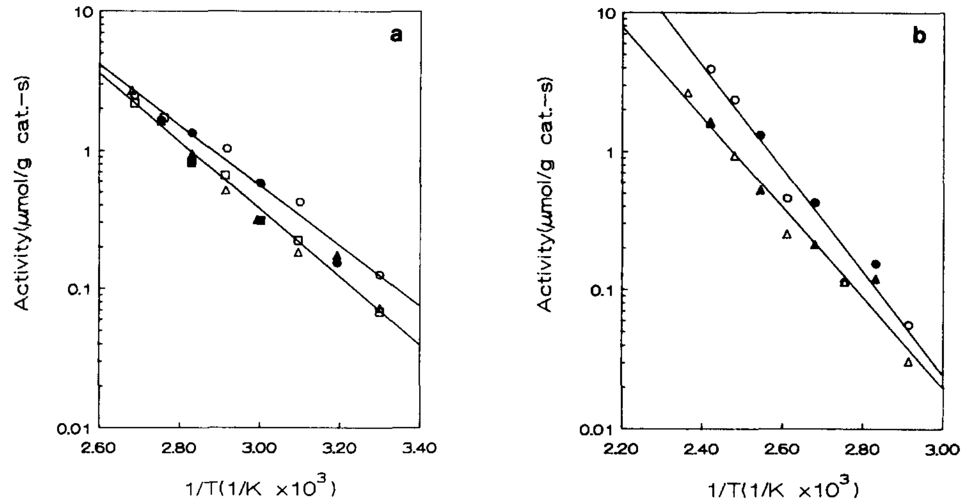

FIG. 1. Arrhenius plots for uncalcined and unreduced 1.8% Pd–11.9% Cu/δ-Al_2O_3 in the absence of water vapor in the feed: Total pressure = 750 Torr, P_{CO} = 26 Torr, P_{O_2} = 132 Torr, balance was He; open symbols, ascending temp.; closed symbols, descending temp. (a) Run 1—circles; Run 2—triangles; Run 3—squares. (b) Run 4—after He treatment at 573 K, circles; Run 5—after calcination at 573 K, triangles.

that for the δ-Al_2O_3-supported catalyst. Originally this catalyst had an activation energy of 8.5 kcal/mole which increased to 10.6 kcal/mole in a second run and to 12.7 kcal/mole in a third consecutive run, as shown in Table 3 and Fig. 2a. The RT activities were 0.0027, 0.0013, and 0.0007 μmol/g cat · s, respectively. These RT activities were not only decreasing with each Arrhenius run but became almost 10 times less

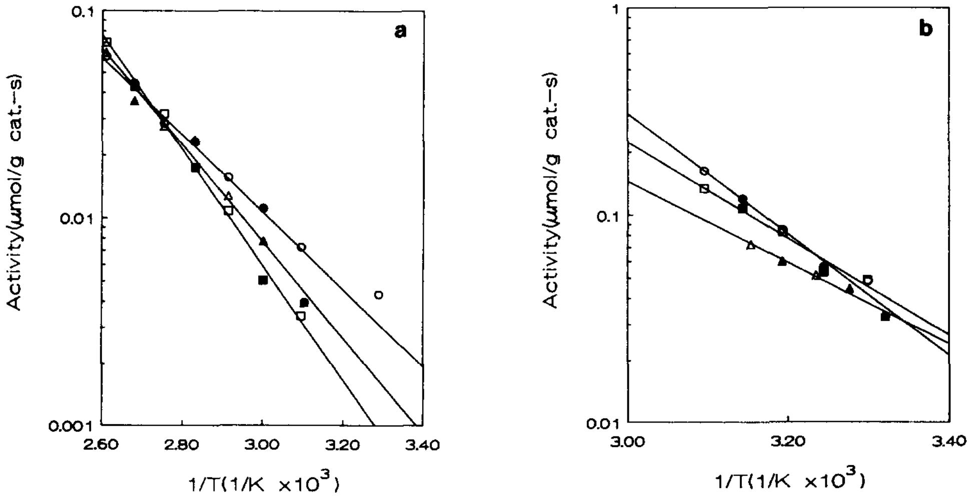

FIG. 2. Arrhenius plots for uncalcined and unreduced 1.8% Pd–11.8% Cu/carbon in the absence of water vapor in the feed: Total pressure = 750 Torr, P_{CO} = 26 Torr, P_{O_2} = 132 Torr, balance was He; open symbols, ascending temp.; closed symbols, descending temp. (a) Run 1—circles; Run 2—triangles; Run 3—after He treatment, squares. (b) Run 4—after He treatment at 573 K, circles; Run 5—after extra He treatment at 673 K, triangles; Run 6—after calcination at 573 K, squares.

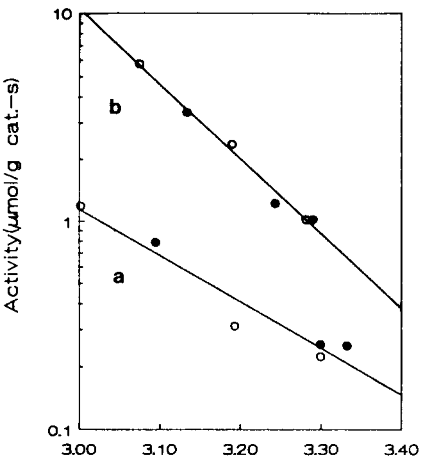

FIG. 3. Arrhenius plots for uncalcined and unreduced 1.8% Pd–11.9% Cu/δ-Al_2O_3 with water vapor in the feed: Total pressure = 750 Torr, P_{CO} = 26 Torr, P_{O_2} = 132 Torr, P_{H_2O} = 5.3 Torr, balance was He; open symbols, ascending temp.; closed symbols, descending temp. (a) Microreactor results. (b) IR reactor results.

than that obtained with the alumina support, as shown in Table 1. This phenomenon can be explained by the adsorption behavior of water vapor on carbon or alumina, and it will be discussed later. However, after drying in flowing He at 573 K for an hour, the RT activity was enhanced to 0.0328 μmole/g cat · s, which seems to be due to the opening of pores filled with water, consequently giving more available surface area for reaction, but the activation energy did not change much (13.3 kcal/mole), as shown in Table 3 and Fig. 2b. An additional drying step in He at 673 K for an hour changed the RT activity little but lowered the activation energy to 7.3 kcal/mole. A final calcination at 573 K (6,000 ppm O_2 in flowing He) for an hour did not change the RT activity but increased the activation energy slightly to 10.6 kcal/mole, as shown in Table 3 and Fig. 2b. After these high temperature steps in He and O_2, the CO pressure dependency exhibited a maximum around 26 Torr, as shown in Fig. 5c.

In the presence of 5.3 Torr H_2O in the feed, the activities were markedly higher (Table 1), and the 1.8% Pd–11.9% Cu/δ-Al_2O_3 catalyst at 303 K now exhibited a negative CO dependency of −0.6 and first-order dependencies on both O_2 and H_2O in either reactor system, as shown in Table 2 and Figs. 5d and 5f. At 323 K, the same negative CO partial pressure dependency of −0.6 was obtained in both reactors, but when the CO pressure dropped below 13 Torr in the microreactor, the dependence changed to give a positive order of 0.7 (Figs. 5d and 5g and Table 2). The dependencies on O_2 remained near first order in both the IR reactor and the microreactor studies. An unusual change in H_2O pressure dependence occurred as the temperature increased to 323 K, as it decreased to 0.1 and 0.5 in the IR reactor and microreactor, respectively. The activation energies in the presence of H_2O were 16 kcal/mole from the IR reactor study and 9.9 kcal/mole from the microreactor study, as shown in Figs. 3a and 3b.

Over the 1.8% Pd–11.8% Cu/carbon catalyst in the presence of water vapor, the activity was markedly enhanced, and positive partial pressure dependencies of 0.8 on CO and 0.6 on O_2 were obtained at 303 K, and a dependency on H_2O vapor of 0.9 at both 303 and 323 K occurred, as shown in Table 2 and Fig. 5h. The initial apparent activation energy for this catalyst was negative, −5.8 kcal/mole, as shown in Fig. 4a. After drying at 573 K in He for an hour, the activity was measured in two sequential runs in the absence of water vapor in the feed. The RT activity was reduced by a factor of 500 while activation energies of 15.0 and 14.2 kcal/mole were obtained (Table 3 and Fig. 4a). Additional drying at 673 K in flowing He further reduced the activity and lowered the activation energy to 12.5 kcal/mole, as in Table 3 and Fig. 4b. A reduction in flowing H_2 for an hour at 573 K reduced the activity by an order of magnitude but did not change the activation energy (12.6 kcal/mole), as shown in Table 3 and Fig. 4b. At the end of these runs, 3 data points were obtained in the presence of water vapor and, as shown

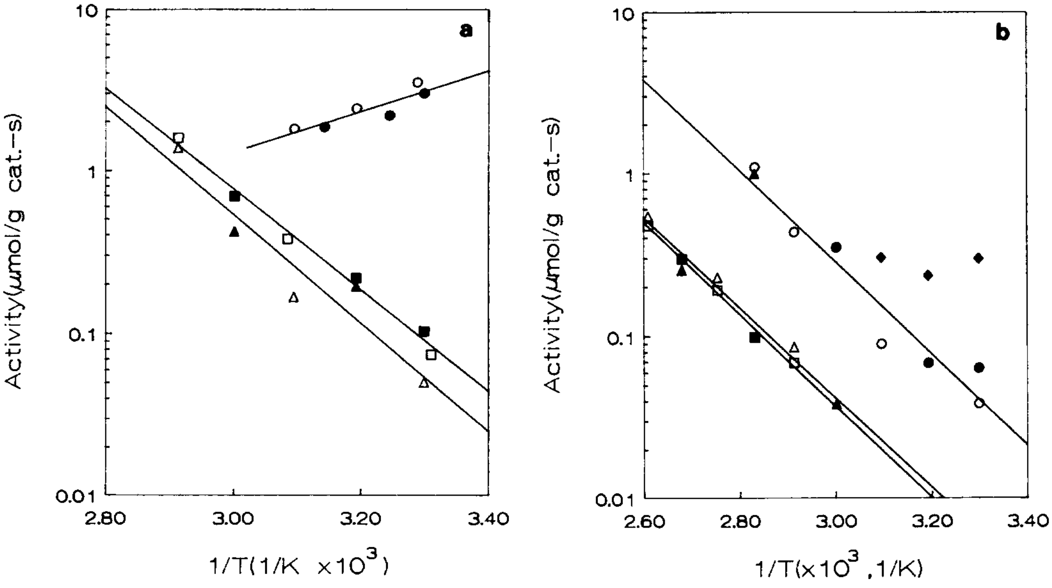

FIG. 4. Arrhenius plots for uncalcined and unreduced 1.8% Pd–11.8% Cu/carbon catalysts: Total pressure = 750 Torr, P_{CO} = 26 Torr, P_{O_2} = 132 Torr, P_{H_2O} = 5.3 Torr, balance was He; open symbols, ascending temp.; closed symbols, descending temp. (a) Run 1—in the presence of H_2O in the feed, circles; Run 2—after drying in He at 573 K (no H_2O in the feed), triangles; Run 3—a repeat of Run 2 with no pretreatment, squares. (b) Run 4—after extra drying in He at 673 K (no H_2O in the feed), circles; Runs 5 and 6—after H_2 reduction at 573 K (absence of H_2O in the feed), triangles and squares; Run 7—in the presence of water vapor in the feed, diamonds.

in Fig. 4b, the activity was greatly enhanced. Over the 0.2% Pd–11.5% Cu/carbon catalyst in the presence of water vapor, a negative apparent activation energy of −7.1 kcal/mole was again obtained, and slightly higher water partial pressure dependencies of 1.2 and 1.5 were obtained at 303 and 323 K, respectively, as shown in Table 2. The 2% Pd–11.8% Cu/carbon catalyst, which was prepared from $PdCl_2$ and $Cu(NO_3)_2$, had lower partial pressure dependencies on both CO and O_2 but a much stronger dependence of 2.5 on H_2O, compared to the catalyst prepared from $PdCl_2$ and $CuCl_2$, as shown in Table 2 and Fig. 5i. However, no stable kinetic behavior was obtained with this catalyst and the activity declined continuously in sequential Arrhenius runs; therefore no activation energy was obtained. This indicates that a catalyst without sufficient chloride cannot carry out the catalytic cycle for CO oxidation effectively, due probably to an insufficient amount of the oxidant, $CuCl_2$. In the presence of 5.3 Torr water vapor, the activity of the carbon-supported catalyst in the microreactor was almost 15 times greater than that of the Al_2O_3-supported catalyst, and it was fivefold higher than the activity of the 1.8% Pd–11.9% Cu/δ-Al_2O_3 wafer in the IR reactor system. This improved performance indicates an important advantage for the use of carbon supports and implies that the amount of adsorbed H_2O plays an important role in CO oxidation. The nearly constant TOF values for the 0.2% Pd and 1.8% Pd carbon-supported catalysts are strong evidence against any diffusional limitations.

IR Results

With the 1.8% Pd–11.9% Cu/δ-Al_2O_3 wafer in the absence of water vapor, IR spectra

TABLE 3

Pretreatment Effect on Catalytic Activities and Apparent Activation Energies for CO Oxidation over Unreduced Pd–Cu Catalysts

Catalyst	P_{H_2O} (Torr)	E_{app}[a] (kcal/mole)	Activity[b] at 300 K (μmole CO/g s × 10^3)	TOF[b,c] at 300 K (s^{-1})	Run seq. or pretreatment[d]
1.8% Pd–11.9% Cu/ δ-Al_2O_3 (IR)	0	10.4 ± 2.6	93.4	0.55	1st KR
	0	11.2 ± 2.7	57.4	0.34	2nd KR (after PR)
	0	11.4 ± 2.7	54.2	0.32	3rd KR
	0	17.0 ± 4.4	1.4	0.008	Drying in He at 573 K for 1 h
	0	14.9 ± 2.5	1.6	0.009	Calcining at 573 K for 1 h
1.8% Pd–11.8% Cu/ Carbon (reactor)	0	8.5 ± 0.1	2.7	0.016	1st KR
	0	10.6 ± 0.1	1.3	0.008	2nd KR
	0	12.7 ± 0.1	0.7	0.004	3rd KR (after PR)
	0	13.3 ± 0.2	32.8	0.19	Drying in He at 573 K for 1 h
	0	7.3 ± 0.1	36.4	0.22	Drying in He at 673 K for 1 h
	0	10.6 ± 0.1	37.4	0.22	Calcining (6000 ppm O_2) at 573 K for 1 h
1.8% Pd–11.8% Cu/ Carbon (reactor)	5.3	−5.8 ± 0.8	1137	6.7	1st KR
	0	15.0 ± 0.7	16.1	0.10	Drying in He at 573 K for 1 h
	0	14.2 ± 0.7	23.6	0.14	Drying in He at 573 K for 1 h
	0	12.5 ± 0.4	12.2	0.07	Drying in He at 673 K for 1 h
	0	12.6 ± 0.2	1.5	0.009	Reducing in H_2 at 573 K for 3 h

[a] Uncertainty is represented by 95% confidence limits.

[b] Standard reaction conditions: P_{O_2} = 132 Torr, P_{CO} = 26 Torr, total P = 750 Torr, dry wt. basis.

[c] TOF = molecule CO reacted per second per Pd atom.

[d] KR represents kinetic run, PR represents partial pressure run.

at low CO pressures of 0.4 and 0.8 Torr were obtained before the CO pressure was increased to 26 Torr CO in He. At 303 K under 0.4 Torr CO pressure, CO bands were obtained at 2158_w, 2120, 2080_{sh}, 1990_m, and 1930 cm^{-1}, as shown in Fig. 6b. An increase to 0.8 Torr CO essentially removed the 2158-cm^{-1} peak (Fig. 6c), as was observed with the Pd-only catalyst in the previous paper (*16*), and this peak never showed up again under CO alone (Fig. 6d). All the other peaks retained their peak positions, and their intensities grew with CO partial pressure, especially the 2120-cm^{-1} band, as shown in Figs. 6b to 6d. However, under reaction conditions at 303 K with 132 Torr O_2 present, the CO band at 2158 cm^{-1} reappeared at the expense of the 1930- and 1990-cm^{-1} peaks, as shown in Fig. 6e. The intensity of the CO band at 2120 cm^{-1} did not change in the presence of O_2. This phenomenon is consistent with our assignment of the 1930-cm^{-1} peak to Pd(I) species and the 2158-cm^{-1} peak to a Pd(II) species (*16*), that

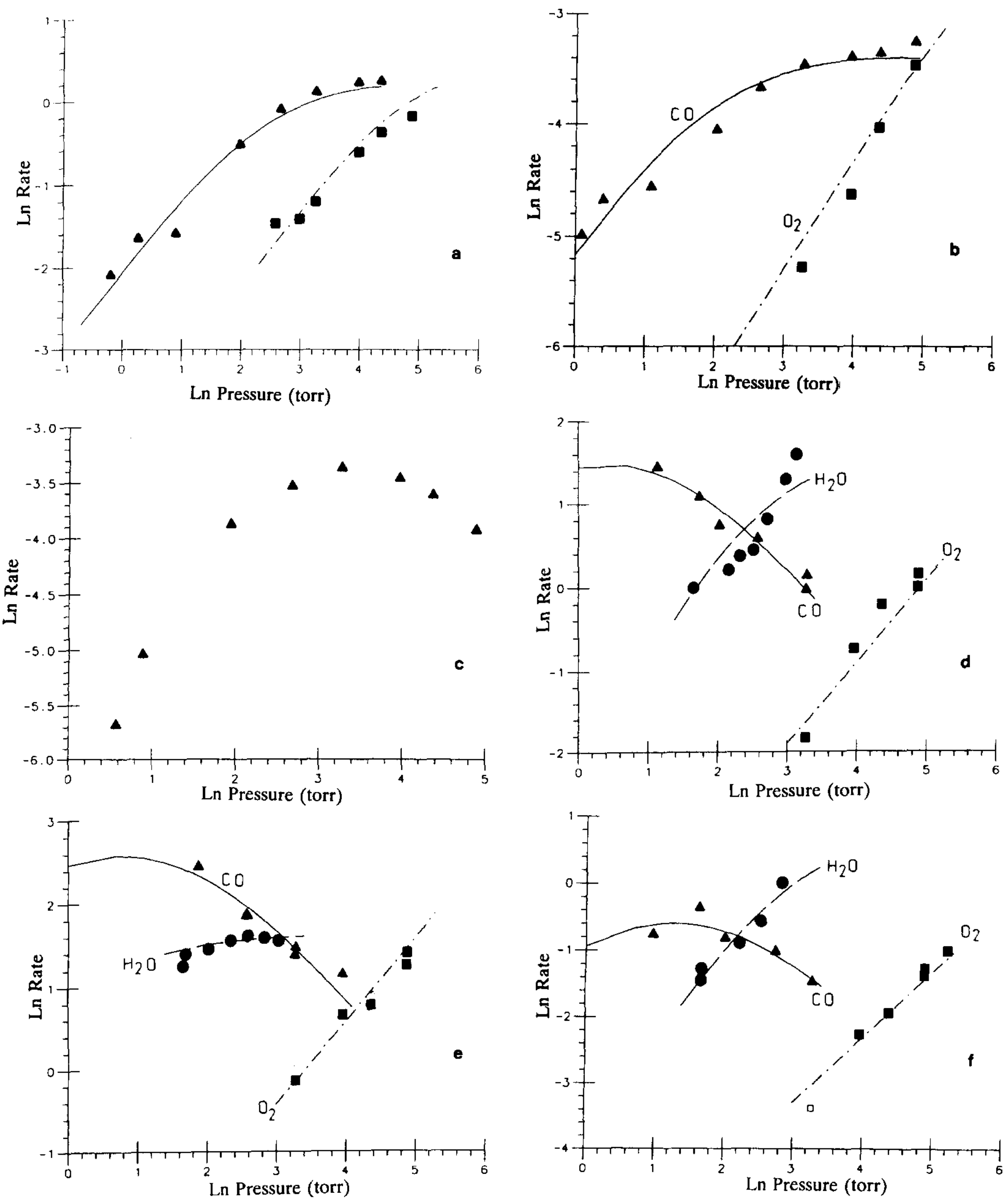

FIG. 5. Comparison between data and results predicted from the model for CO oxidation over Pd–Cu catalysts: CO, ▲; O_2, ■; H_2O, ●; lines are computer fitted. (a) 1.8% Pd–11.9% Cu/δ-Al_2O_3 at 353 K without H_2O in the feed(IR). (b) 1.8% Pd–11.8% Cu/C at 363 K without H_2O in the feed(reactor). (c) 1.8% Pd–11.8% Cu/C at 303 K without H_2O in the feed(reactor). (d) 1.8% Pd–11.8% Cu/δ-Al_2O_3 at 303 K with H_2O in the feed (IR). (e) 1.8% Pd–11.9% Cu/δ-Al_2O_3 at 323 K with H_2O in the feed(IR). (f) 1.8% Pd–11.9% Cu/δ-Al_2O_3 at 303 K with H_2O in the feed(reactor). (g) 1.8% Pd–11.9% Cu/δ-Al_2O_3 at 323 K with H_2O in the feed(reactor). (h) 1.8% Pd–11.5% Cu/C at 303K with H_2O in the feed(reactor). (i) 2% Pd–11.8% Cu/C at 303 K with H_2O in the feed(reactor). (Prepared from $PdCl_2$ and $Cu(NO_3)_2 \cdot 5H_2O$.) P_{CO} = 26 Torr when P_{O_2} or P_{H_2O} varied. P_{O_2} = 131 Torr when P_{CO} or P_{H_2O} varied. P_{H_2O} = 5.3 Torr when P_{CO} or P_{O_2} varied.

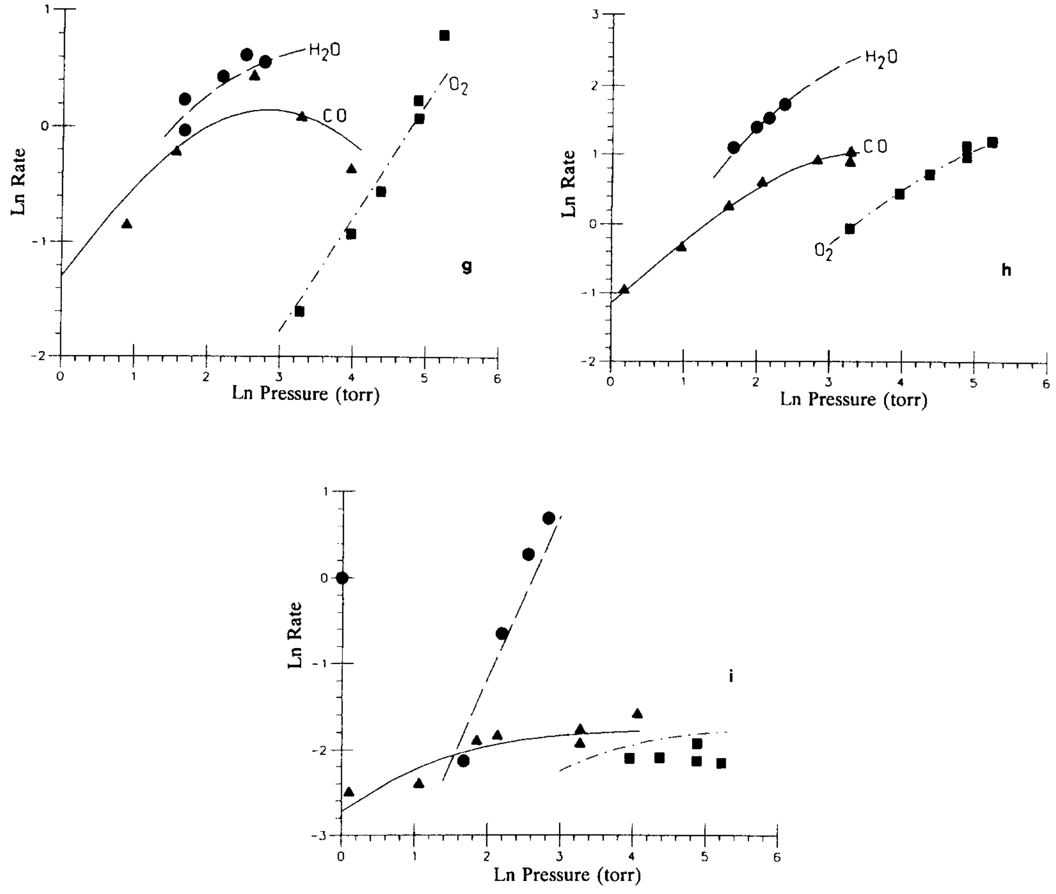

FIG. 5—*Continued*

is, the Pd(I) species are converted to Pd(II) in the presence of O_2. Under reaction conditions at 353 K, the intensities of all the peaks grew with increasing CO pressure, as shown in Figs. 6f to 6h, except for the 2158-cm^{-1} peak, whose intensity was independent of CO pressure. Figs. 6i to 6k show that the 2158-cm^{-1} peak intensity gradually increased and the 1930-cm^{-1} peak intensity decreased as O_2 pressure increased. The intensity of the CO band at 2120 cm^{-1}, which is assigned to a Cu(I) species, decreased as O_2 pressure increased. This trend of change in peak intensity is consistent with expectations as the amount of Cu(I) species should be decreased because of its increased oxidation to Cu(II) species.

The IR spectra in the presence of H_2O were obtained with a different wafer pressed from the same 1.8% Pd–11.9% Cu/δ-Al_2O_3 catalyst, and the same peaks in the presence of CO alone were again obtained, as shown in Fig. 7b. With the addition of 5.3 Torr of water vapor to the feed, the 1930-cm^{-1} band was markedly decreased and only a shallow, broad band existed between 1800 and 2000 cm^{-1}, along with a weak 1990-cm^{-1} peak (Fig. 7c). The addition of 132 Torr O_2 restored the 1930-cm^{-1} band, and both it and the 1990-cm^{-1} band were near their original intensities. However, the 2120-cm^{-1} peak intensity decreased only slightly upon the introduction of either water or oxygen. At 303 K, the 1930- and 2120-cm^{-1} peak intensities, particularly the latter, decreased as the CO pressure decreased, as shown in Figs.

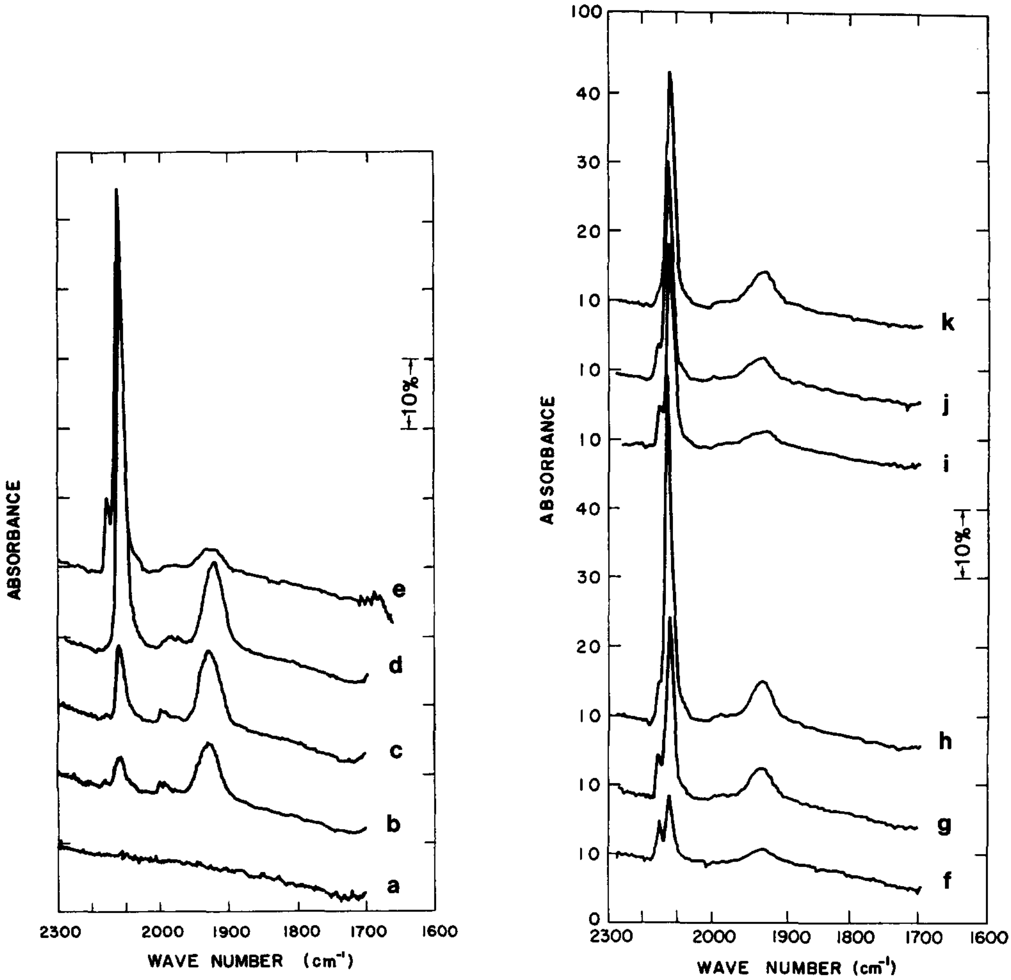

FIG. 6. Sequential IR spectra of 1.8% Pd–11.9% Cu/δ-Al_2O_3 in the absence of water vapor in the feed: Gas flow = 28.5 cm^3/min, total pressure = 750 Torr. (a) He only at 303 K. (b) He + 0.4 Torr CO at 303 K. (c) He + 0.8 Torr CO at 303 K. (d) He + 26 Torr CO at 303 K. (e) He + 26 Torr CO + 132 Torr O_2 at 303 K. (f) He + 6.6 Torr CO + 132 Torr O_2 at 353 K. (g) He + 26 Torr CO + 132 Torr O_2 at 353 K. (h) He + 79 Torr CO + 132 Torr O_2 at 353 K. (i) He + 26 Torr CO + 132 Torr O_2 at 353 K. (j) He + 26 Torr CO + 79 Torr O_2 at 353 K. (k) He + 26 Torr CO + 13 Torr O_2 at 353 K.

7d to 7f. All the peak intensities decreased simultaneously as the O_2 pressure was decreased, as shown in Figs. 7g to 7i, and this pattern was unanticipated. As the water vapor pressure increased, the peak intensities decreased only slightly (Figs. 7j to 7l). At 323 K, a somewhat different dependence on O_2 was found as band intensities first increased then decreased as the O_2 pressure was lowered, as indicated in Figs. 7m to 7o. With increasing water vapor pressure, the 2120-cm^{-1} peak intensity decreased continuously while the 1930- and 1990-cm^{-1} peaks showed a small increase before declining, as shown in Figs. 7p to 7r. The trend with CO pressure was identical to that at 303 K.

DISCUSSION

Band Assignments

Band assignments for Pd and Cu species in Pd-only and Cu-only catalysts were made

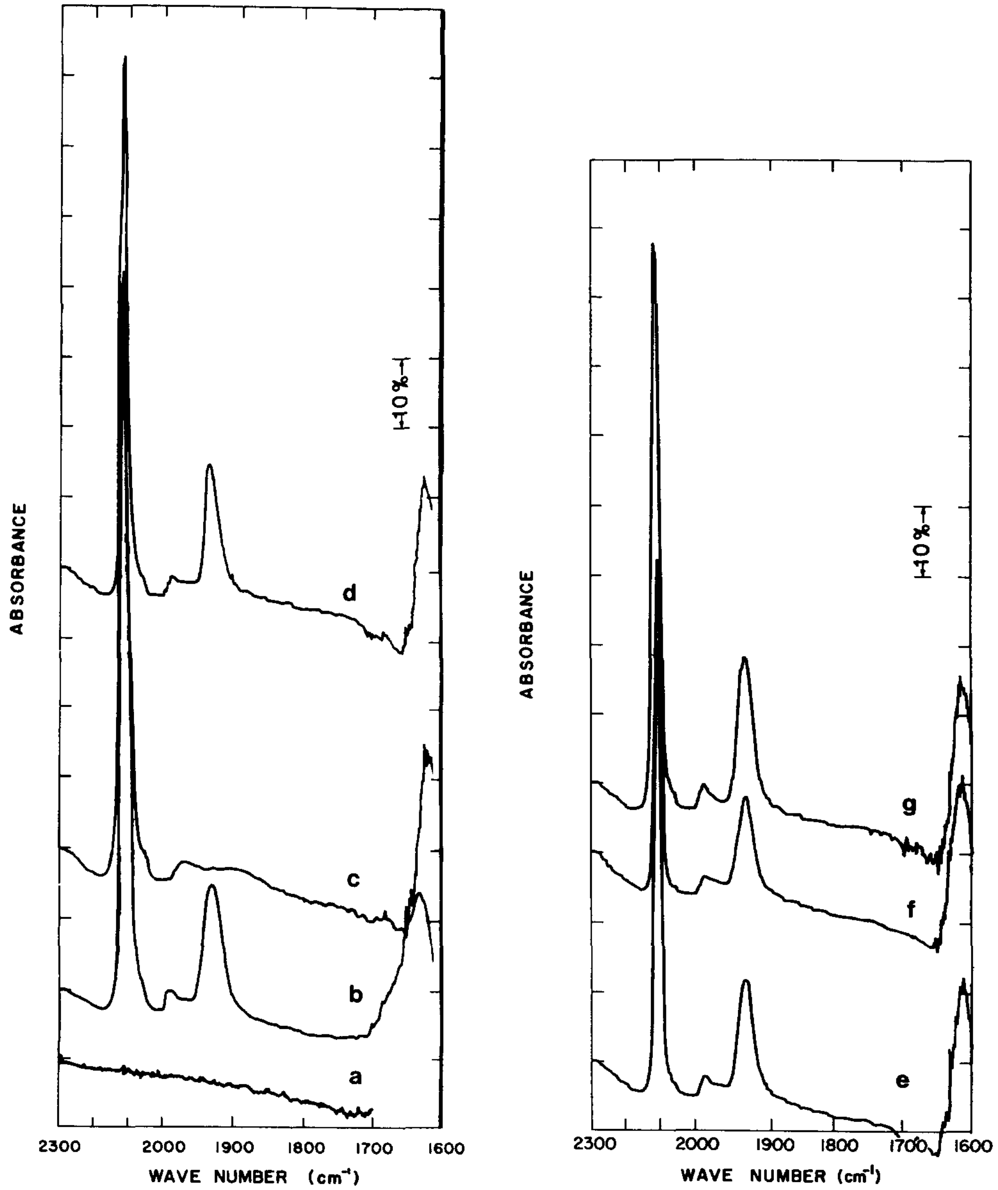

FIG. 7. Sequential IR spectra of 1.8% Pd–11.9% Cu/δ-Al_2O_3 with water vapor in the feed. Gas flow = 28.5 cm^3/min, total pressure = 750 Torr. (a) He only at 303 K. (b) He + 26 Torr CO at 303 K. (c) He + 26 Torr CO + 5.3 Torr H_2O at 303 K. (d) He + 26 Torr CO + 5.3 Torr H_2O + 132 Torr O_2 at 303 K. (e) He + 13 Torr CO + 5.3 Torr H_2O + 132 Torr O_2 at 303 K. (f) He + 6.6 Torr CO + 5.3 Torr H_2O + 132 Torr O_2 at 303 K. (g) He + 26 Torr CO + 5.3 Torr H_2O + 132 Torr O_2 at 303 K. (h) He + 26 Torr CO + 5.3 Torr H_2O + 79 Torr O_2 at 303 K. (i) He + 26 Torr CO + 5.3 Torr H_2O + 26 Torr O_2 at 303 K. (j) He + 26 Torr CO + 5.3 Torr H_2O + 132 Torr O_2 at 303 K. (k) He + 26 Torr CO + 7.5 Torr H_2O + 132 Torr O_2 at 303 K. (l) He + 26 Torr CO + 10.4 Torr H_2O + 132 Torr O_2 at 303 K. (m) He + 26 Torr CO + 5.3 Torr H_2O + 132 Torr O_2 at 323 K. (n) He + 26 Torr CO + 5.3 Torr H_2O + 79 Torr O_2 at 323 K. (o) He + 26 Torr CO + 5.3 Torr H_2O + 26 Torr O_2 at 323 K. (p) He + 26 Torr CO + 5.3 Torr H_2O + 132 Torr O_2 at 323 K. (q) He + 26 Torr CO + 7.6 Torr H_2O + 132 Torr O_2 at 323 K. (r) He + 26 Torr CO + 10.6 Torr H_2O + 132 Torr O_2 at 323 K.

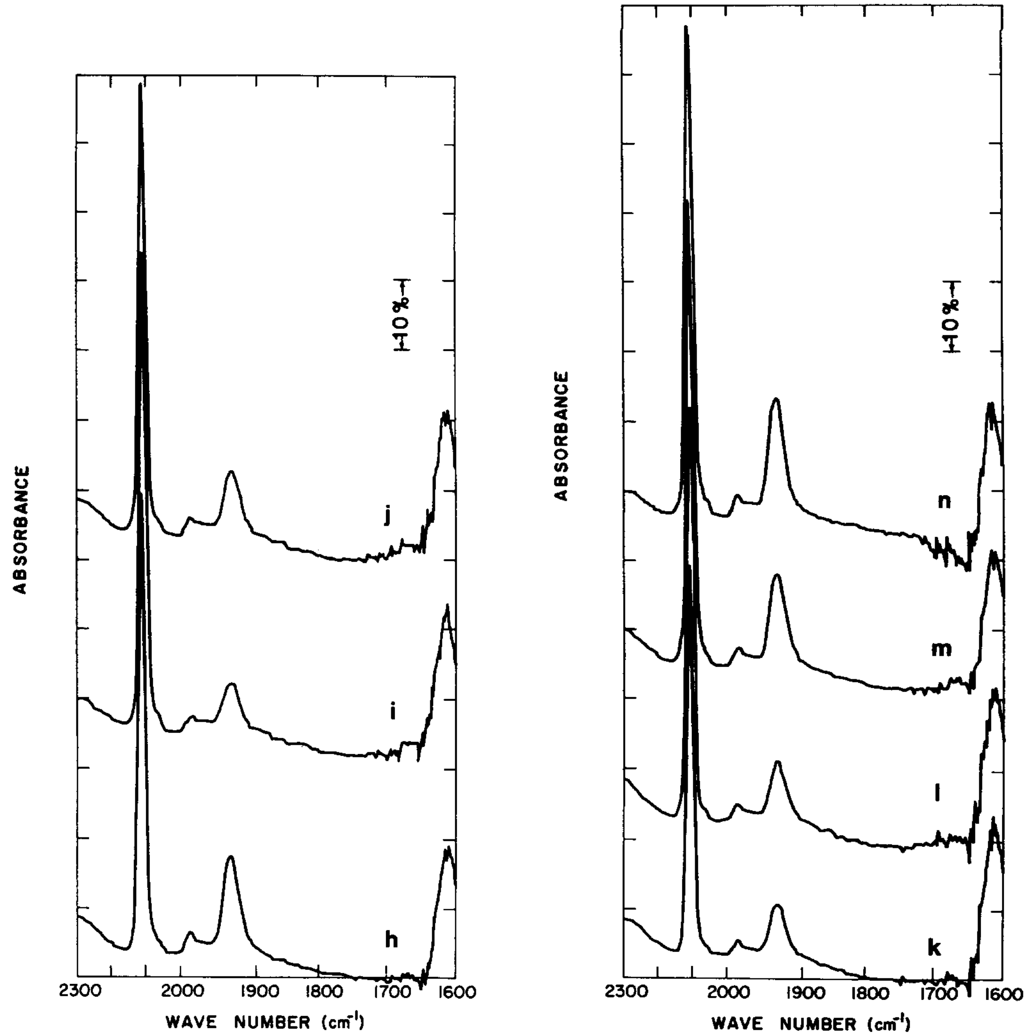

FIG. 7—*Continued*

in the previous paper based upon spectra reported in the literature (*16*), thus it is relatively straightforward to assign the peaks in the Pd–Cu system as no new bands were observed. It is clear that the 2120-cm^{-1} peak is associated with a Cu(I)–CO complex, and the 2080_{sh}-, 1990-, and 1930-cm^{-1} peaks are related to Pd–CO complexes. The 2080_{sh}-cm^{-1} peak can be assigned to CO terminally adsorbed on palladium metal surfaces, as was done with the Pd-only catalysts (*16*). The assignment of the two peaks at 1990 and 1930 cm^{-1} could be ambiguous because their positions agree well with bands reported for bridged carbonyls in Pd(I) compounds as well as those for bridge-bonded CO on metallic Pd surfaces. However, the behavior of these two peaks in the presence of water was the same as that observed for the Pd-only catalyst, namely, the intensity of the 1930-cm^{-1} band did not vary in concert with the 2080-cm^{-1} band (*16*). There-

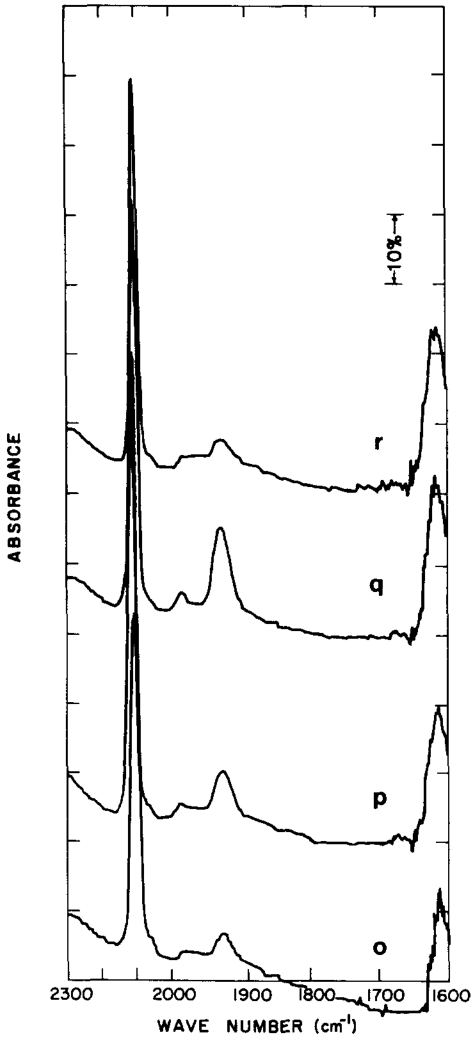

FIG. 7—*Continued*

fore, the same assignments for the Pd–CO species in Pd–Cu bimetallic systems can be made as in the Pd-only catalyst, i.e., the 2080- and 1990-cm^{-1} bands are associated with linear and bridge-bonded CO on palladium metal surfaces, respectively, and the 1930-cm^{-1} band is associated with bridged carbonyl ligands in Pd(I) complexes such as the $(PdCOCl)_n$ species, which can polymerize via bridged CO ligands (*17*). However, it is possible that the band at 1990 cm^{-1} may also be associated with CO in Pd(I) complexes because its intensity decreased simultaneously with the 1930-cm^{-1} peak as the O_2 pressure decreased, as indicated in Figs. 7f to 7h. Consequently, both the 1930- and 1990-cm^{-1} peaks may contain contributions from CO adsorbed on Pd metal and carbonyls associated with Pd(I) species although the latter should dominate, particularly since the two observed bands are much narrower than those typically obtained for CO on metallic Pd surfaces. The strongest peak in the spectrum at 2120 cm^{-1} is undoubtedly CO associated with Cu(I), i.e., the CuCOCl species, as observed in the Cu-only catalyst (*16*). Because of the high Cu/Pd mole ratio of 10, a much stronger peak for the CuCOCl species is expected compared to those for the Pd–CO species.

Kinetic Behavior

Studies of CO oxidation on unreduced bimetallic catalysts, especially on $PdCl_2$–$CuCl_2$ catalysts, have been conducted by Desai *et al.* (*1, 2*) on alumina-supported $PdCl_2$–$CuCl_2$ and Golodov *et al.* (*3–7*) on this bimetallic system in aqueous solution. Both groups have shown that $PdCl_2$–$CuCl_2$ systems have a very high activity for CO oxidation compared to other CO oxidation catalysts, and they are very active even at room temperature. Desai *et al.* (*1, 2*) proposed a reaction mechanism quite similar to that proposed for the Wacker process (*8, 9*), which is used to oxidize ethylene to acetaldehyde. The overall chemistry for CO oxidation they proposed is

$$CO + PdCl_2 + H_2O \rightarrow CO_2 + Pd^{(0)} + 2HCl \quad (1)$$

$$Pd^{(0)} + 2CuCl_2 \rightarrow PdCl_2 + 2CuCl \quad (2)$$

$$4CuCl + 4HCl + O_2 \rightarrow 4CuCl_2 + 2H_2O \quad (3)$$

Pd(II) is reduced to Pd(0) in reaction (1) and then Pd(0) is reoxidized in reaction (2) by $CuCl_2$, and the resulting CuCl is finally reoxidized by molecular oxygen in reaction (3). In the kinetic rate expression they propose, the reaction order is unity with respect to CO and minus one-half with respect to O_2.

For the $PdCl_2$–$CuCl_2$ system in aqueous solutions, Golodov *et al.* (*3–7*) proposed the following different reaction mechanism:

either

$$[PdCl_4]^{-2} + O_2 \rightleftharpoons [PdCl_3O_2]^- + Cl^- \quad (4)$$

$$[PdCl_3O_{2]}^- + CO \rightleftharpoons [PdCl_3CO]^- + O_2 \quad (5)$$

or

$$[PdCl_4]^{-2} + CO \rightleftharpoons [PdCl_3CO]^- + Cl^- \quad (6)$$

then

$$[PdCl_3CO]^- + 2CuCl_2(H_2O)_2 \xrightarrow[-H_2O]{} [PdCl_4]^{-2} + 2CuCl + CO_2 + Cl^- + 2H^+ \quad (7)$$

or

$$[PdCl_3CO]^- + CuCl_2(H_2O)_2 + CO \rightarrow PdClCO + CuCl + CO_2 + 3Cl^- + 2H^+ \quad (8a)$$

followed by

$$PdClCO + CuCl_2 \xrightarrow{\text{fast}} PdCl_2CO + CuCl \quad (8b)$$

$$CuCl + CO \rightarrow CuCOCl \quad (9)$$

$$CuCOCl + PdCl_4{}^{-2} \xrightarrow{\text{slow}} [PdCl_3CO]^- + Cl^- + CuCl \quad (10)$$

Reactions (9) and (10) are autocatalytic reactions initiated by CuCl, and thus a Cu species is also involved in the activation of CO. They observed that the reaction rate decreases with increasing P_{O_2}, which was explained by assuming that oxidation of the active species, CuCl, to $CuCl_2$ occurred. In their derived rate expression for aqueous solutions, the predicted partial pressure dependencies on CO and O_2 were unity and zero, respectively, with first-order dependencies on both Pd(II) and Cu(I) species.

As mentioned earlier, Zhizhina *et al.* (*11–14*) have also studied CO oxidation in aqueous solutions of $PdCl_2$ with various oxidants; however, they concluded that Pd(I) carbonyl complexes were the active catalytic species in this reaction, and their proposed mechanism is given by the set of reactions

$$Pd^{(II)} + CO + H_2O \xrightarrow{\text{slow}} Pd^{(0)} + CO_2 + 2H^+ \quad (11)$$

$$Pd^{(0)} + Pd^{(II)} + CO \rightleftharpoons Pd_2^{(I)}(CO) \quad (12)$$

$$Pd_2^{(I)}(CO) + Ox. \xrightarrow{\text{fast}} Pd^{(II)} + Pd^{(0)} + CO_2 + Red. \quad (13)$$

$$Pd^{(0)} + Ox. \rightarrow Pd^{(II)} + Red. \quad (14)$$

where Ox. is the oxidizing agent and Red. is the reduced oxidant.

The role of water in CO oxidation was also examined by Desai *et al.* (*1, 2*) and Kuznetsova *et al.* (*14*). Desai *et al.* observed that when the feed was dry, the conversion during the stable period was about 12%, but once the feed was switched to a wet gas (55 Torr H_2O), the conversion reached a stable conversion near 64%. Kuznetsova *et al.* suggested that active complexes might be formed by an interaction with water.

Reaction Mechanism over Supported $PdCl_2$–$CuCl_2$ Catalysts without Water Vapor in the Feed

As shown previously, $PdCl_2$ and $CuCl_2$ species can be easily reduced to Pd(I) and Cu(I) species in the presence of CO and water adsorbed on the support surface (*16*). These same Pd(I) and Cu(I) carbonyl complexes were identified in the bimetallic catalysts by IR spectroscopy, as shown in Figs. 6b and 6d, for example. Therefore the same initial reaction steps can be expected to occur and an overall reaction sequence is proposed as follows:

$$2PdCl_2 + CO + H_2O_{ad} \xrightleftharpoons{K_1} 2PdCl + CO_2 + 2HCl_{ad} \quad (15)$$

$$2CuCl_2 + CO + H_2O_{ad} \xrightleftharpoons{K_1'}$$

$$2CuCl + CO_2 + 2HCl_{ad} \quad (16)$$

$$PdCl + CO \overset{K_{CO}}{\rightleftharpoons} PdClCO \quad (17)$$

$$CuCl + O_2 \overset{K'_{O_2}}{\rightleftharpoons} CuClO_2 \quad (18)$$

$$CuCl + CO \overset{K'_{CO}}{\rightleftharpoons} CuClCO \quad (19)$$

$$PdCl + O_2 \overset{K_{O_2}}{\rightleftharpoons} PdClO_2 \quad (20)$$

$$CuClCO + PdClO_2 \overset{K_2}{\rightleftharpoons} \underset{\text{I}}{PdCuCl_2(CO)O_2} \quad (21)$$

$$\underset{\text{I}}{PdCuCl_2(CO)O_2} \xrightarrow{k_3,\ \text{rds}} CuCl + CO_2 + OPdCl \quad (22)$$

$$OPdCl + CO \overset{K_4}{\rightleftharpoons} PdCl + CO_2 \quad (23)$$

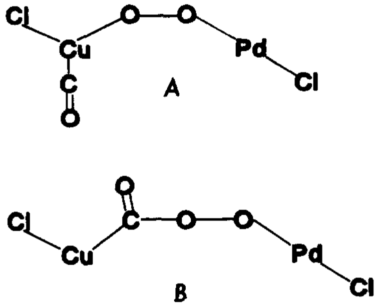

FIG. 8. A possible structure of intermediate [I] proposed by analogy with $[(NH_3)_5CoOOCo(NH_3)_5]^{4+}$ or $[(NH_3)_5CoOOCo(NH_3)_5]^{5+}$ species (*22, 23*).

This is the mechanism associated with the *initial* low-temperature activity, and this sequence of steps involves only the water initially present from the impregnation step, i.e., that in the first reaction (Eq. (15)). The first four steps establish the catalytic species and the catalytic cycle is composed of the final five steps. Step (16) was proposed by Dontsova (*18*) and Byerley and Lee (*19*) many years ago, and justification of step (21) comes from the work of Sun and Cheng (*20, 21*), who suggested that Cu(I) carbonyls play a role in supplying CO to a $Pt_2Cl_2(CO)_2$ complex when CO is dissolved in aqueous solutions. Intermediate [I] is similar to the one proposed in the previous paper (*16*) with an O_2^{-2} bridge between Cu(I) and Pd(II), as depicted in Fig. 8a, and during decomposition it could pass through the configuration in Fig. 8b as the work of Fronczek *et al.* (*22*) and Vannerberg and Brosset (*23*) on Co–O_2 complexes provides precedent for this configuration. Golodov *et al.* (*5*) have also proposed a Pd–Cu species containing CO and Cl. The rupture of the O–O bond in intermediate [I] is assumed to be the rate determining step (rds), as shown in step (22). Again, as with the Pd-only catalysts, the rapid formation of the 1930-cm^{-1} peak (PdCOCl), the concomitant evolution of CO_2 measured by gas chromatography during the initial introduction of CO, and the increase in the 1930-cm^{-1} peak as the CO pressure increases support the proposal of the quasi-equilibrated steps preceding the rds step in step (22). The rate equation derived from this model is discussed later.

Reaction Mechanism over Supported $PdCl_2$–$CuCl_2$ Catalysts with Water Vapor in the Feed

The previous studies of CO oxidation using Pd–Cu catalysts have usually shown a first-order dependency on CO and a zero-order dependency on O_2 although Desai *et al.* (*1, 2*) observed a negative half-order dependency on O_2 over their chlorinated $PdCl_2$–$CuCl_2$/δ-Al_2O_3 catalyst. Our study has found different, more complicated partial pressure dependencies on CO, O_2, and H_2O vapor, i.e., both positive and negative reaction orders for CO have been observed, positive orders have varied from one-half to one for O_2, and a variation in the reaction order on H_2O from approximately one to two has occurred. However, another study from the laboratory in which Desai worked reported reaction orders for CO and O_2 similar to those found in this study, i.e., a catalyst used by Heriquez (*24*) consisted of $PdCl_2$, $CuCl_2$, and $Cu(NO_3)_2$ dissolved in water and dispersed on alumina, and the rate expression had a negative half-order dependency on CO and a first-order dependency on O_2.

Because of the *in situ* IR spectra obtained in this study, the reaction mechanism proposed here has more constraints, and it must be consistent with the following experimental observations:

(1) Both negative- and positive-order dependencies on CO can occur;

(2) only positive dependencies on O_2 exist;

(3) water vapor pressure dependencies are positive and can be higher than first order;

(4) dependency on Pd is first order;

(5) certain changes in IR peak intensities are induced by the reactants.

As with the Pd-only catalysts, the sequence of steps proposed for CO oxidation in the presence of H_2O vapor is very similar to the chemistry proposed in its absence, yet there are some notable differences to explain the marked rate enhancement that is observed when water vapor is added. The explanations are similar to those proposed for the Pd-only catalysts in the previous paper (*16*); however, due to the presence of the copper, there is a difference in that the rate determining step (rds) now shifts from the reoxidation of Pd(0) by O_2 to the reoxidation of Cu(I) to Cu(II) by dioxygen. This is proposed because of the rapidity of interaction between water and the Pd–chlorocarbonyl species observed (step 32)). This assumption gives the first-order dependency on O_2 observed experimentally. In addition to the high reactivity of molecular water with the $[PdClCO]_n$ species to give CO_2 and hydrogen, a reaction which is similar to the water gas shift reaction, the large activity increase in the presence of low concentrations of H_2O can also be attributed to a larger solubilized fraction of the $PdCl_2$ and $CuCl_2$ precursors. Although the reaction between PdClCO and $PdClO_2$ proposed for the Pd-only catalysts can still occur to give CO_2, its contribution to the overall rate is now inconsequential. The proposed mechanism describing CO oxidation in the presence of water vapor is

$$H_2O_{(g)} \overset{K_{H_2O}}{\rightleftharpoons} H_2O_{(ad)} \qquad (24)$$

$$PdCl_2 + H_2O_{ad} \overset{K_1}{\rightleftharpoons} PdCl_{2(aq)} \qquad (25)$$

$$2PdCl_{2(aq)} + CO + H_2O_{(ad)} \overset{K_2}{\rightleftharpoons} \underset{\text{I}}{2PdCl_{(aq)}} + CO_2 + 2HCl_{(ad)} \qquad (26)$$

$$2CuCl_{2(aq)} + CO + H_2O_{(ad)} \overset{K_3}{\rightleftharpoons} 2CuCl_{(aq)} + CO_2 + 2HCl_{(ad)} \qquad (27)$$

$$CuCl_{(aq)} + O_2 \overset{K'_{O_2}}{\rightleftharpoons} CuClO_{2(aq)} \qquad (28)$$

$$PdCl_{(aq)} + CO \overset{K_{CO}}{\rightleftharpoons} PdClCO_{(aq)} \qquad (29)$$

$$PdCl_{(aq)} + O_2 \overset{K_{O_2}}{\rightleftharpoons} PdClO_{2(aq)} \qquad (30)$$

$$CuCl_{(aq)} + CO \overset{K'_{CO}}{\rightleftharpoons} CuClCO_{(aq)} \qquad (31)$$

$$PdClCO_{(aq)} + H_2O_{(ad)} \overset{K_4}{\rightleftharpoons} Pd^{(0)} + CO_2 + HCl_{(aq)} + \tfrac{1}{2}H_{2(aq)} \qquad (32)$$

$$Pd^{(0)} + CuCl_{2(aq)} \overset{K_5}{\rightleftharpoons} PdCl_{aq} + CuCl_{(aq)} \qquad (33)$$

$$CuClCO_{(aq)} + PdClO_{2(aq)} \overset{K_6}{\rightleftharpoons} \underset{\text{I}}{PdCuCl_2(CO)O_{2(aq)}} \qquad (34)$$

$$\underset{\text{I}}{PdCuCl_2(CO)O_{2(aq)}} \xrightarrow{k_7,\ \text{rds}} \underset{\text{II}}{PdCuCl_2O_{(aq)}} + CO_2 \qquad (35)$$

$$\underset{\text{II}}{PdCuCl_2O_{(aq)}} + HCl_{(ad)} + \tfrac{1}{2}H_{2(aq)} \overset{K_8}{\rightleftharpoons} CuCl_{2(aq)} + PdCl_{(aq)} + H_2O \qquad (36)$$

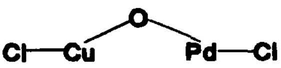

FIG. 9. A possible structure of intermediate [II] proposed in Eq. (35).

Although some of these steps are speculative, they are consistent with published studies. The inclusion of this detail in the reaction sequence is not required for the determination of a rate expression, but these steps can provide insight into the reaction mechanism and can provide suggestions for testing it.

The first eight steps establish the Pd(I) and Cu(I) species on the surface and the catalytic cycle is represented by the last eight steps. It was mentioned in the previous chapter that direct reoxidation of Pd(0) with dioxygen can be difficult, but it is known to be facilitated by an oxidant like $CuCl_2$, and the rate of Pd reoxidation is much faster in Pd–Cu catalysts. However, reoxidation of Cu(I) to Cu(II) now seems to be much slower than the other steps in the catalytic cycle, and it has been assumed to be the rate determining process. This is also the only assumption we have found that provides a first-order O_2 dependence. Although the mechanism of the oxidation of Cu(I) to Cu(II) is not known, because of the strength of the CuClCO IR peak, it has been assumed that this is the Cu(I) species most likely to be oxidized. Furthermore, if Pd is considered as a catalyst to help activate oxygen, one possible sequence is suggested in steps (34–36). The intermediate [I] again exists, and intermediate [II] may have the configuration shown in Fig. 9.

The principal difference between the reaction mechanisms for the Pd-only catalyst and the Pd–Cu catalyst is the chemistry associated with the oxidation of Pd(0) to Pd(I). With only Pd in the presence of H_2O, metallic Pd was presumed to be oxidized via palladium–oxygen complexes, whereas when $CuCl_2$ is also present, zero-valent Pd can be oxidized by $CuCl_2$, as in step (33), and CuCl is reoxidized to $CuCl_2$ by O_2, possibly as shown in steps (34) to (36). The redox sequence has been well-established in the Wacker process, and the more rapid regeneration of the catalytically active Pd(I) species can account for the higher activities.

Water is clearly very important for the achievement of large rate enhancements, and it contributes both as a solvent for the Pd and Cu complexes and as a reactant to form CO_2 as shown in step (32), which will have a net reaction rate equal to that of the rds. However, it may also play an additional role as a ligand in some of these complexes whose coordinative unsaturation could be relieved by ligation to water or hydroxyl groups. One aspect of this reaction that has not yet been completely determined is the source of oxygen in the reaction product, CO_2, i.e., it can come from either dioxygen or water in the catalytic cycle shown previously. Zudin *et al.* (*25*) used isotopically labeled oxygen and water to investigate the mechanism of CO oxidation in the presence of Pd–phosphine complexes in solution. They found that the oxygen atom in CO_2 came from water in acidic solutions and from molecular oxygen in neutral solutions. Our catalysts were prepared from HCl solutions and the chloride resides on the surface; therefore, the adsorbed water layer would be expected to be acidic, thus the results are consistent with the work of Zudin *et al.*

The IR results support this reaction model as Fig. 7c shows a sharp decrease in the 1930-cm^{-1} peak for PdClCO upon addition of water vapor, and the evolution of CO_2 during this period further supports the quasi-equilibrated reaction described in step (26). In the absence of water vapor, the carbonyl band at 2158 cm^{-1}, associated with CO coordinated with Pd(II), was observed as shown in Fig. 6; however, it was not detected in the presence of water vapor. These latter IR results are also consistent with our model as step (15) implies that Pd(II) may not be fully reduced to Pd(I) if insufficient water is present. Therefore, the addition of water vapor forces the further conversion of Pd(II) species to Pd(I) complexes and decreases the concentration of Pd(II) carbonyl complexes below IR spectroscopic detection limits.

The presence of tiny amounts of metallic palladium is indicated by the bands at 2090 and 1990 cm^{-1} although they did not grow when water was added. Figure 7d shows that the 1930-cm^{-1} peak recovered its original intensity upon the addition of O_2, which indicates that $[PdClCO]_n$ species were reformed and are present under reaction conditions. As this behavior was not observed over Pd-only catalysts, it is quite clear that the presence of Pd(I) carbonyl species is favored when Cu species exist in the catalyst and O_2 is present in the feed stream. This observation is similar to chemistry in the Wacker process in which Pd metal is reoxidized to Pd(II) by $CuCl_2$ via a redox sequence involving CuCl and O_2, as stated in Eqs. (2) and (3). However, only a one-electron redox sequence to give Pd(I) is needed in our sequence, as this appears to be the major catalytic species, in agreement with Zhizhina *et al.* (*11–14*). The increase in the 1930-cm^{-1} band for PdClCO as O_2 pressure increases (Figs. 6 and 7) is consistent with this proposal. It also provides some of the strongest evidence against assigning this peak to CO adsorbed on metallic Pd. This redox chemistry is well known in $PdCl_2$–$CuCl_2$ systems, and it is surprising that no IR studies of this chemistry have been reported.

One unexplained trend remains in this complicated system—the increase in the peak intensity for CuClCO (2120 cm^{-1}) at 303 K as the O_2 partial pressure increases, as shown in Figs. 7g to 7i, and also at 323 K as in Figs. 7m to 7o. It might be expected that the greater the O_2 partial pressure, the greater the degree of oxidation of Cu(I) to Cu(II); therefore, the amount of Cu(I) would decrease with increasing O_2 partial pressure. In the absence of water vapor, this behavior occurs, as demonstrated in Figs. 6i to 6k. However, a complex set of equilibria exists which involves $CuCl_2$, H_2O, and oxygen, that is, Eqs. (16), (29), and (31), and predictions are not straightforward. Also, the possibility that the $PdCuCl_2(CO)O_2$ species may have a band overlapping the 2120-cm^{-1} band cannot be discounted.

The two reaction mechanisms—in either the presence or absence of vapor-phase water—are consistent with our IR and kinetic results, but they differ from those proposed previously (*1–7, 11–14*), as mentioned earlier in this discussion. Such differences are not surprising because the metal precursors, the supports, the catalyst systems, and the catalyst pretreatments have varied. The catalyst studied by Desai *et al.* (*1, 2*) had been prepared from $CuCl_2 \cdot 2H_2O$, $Cu(NO_3)_2 \cdot 3H_2O$, and $PdCl_2$, but in this study only $CuCl_2$ and $PdCl_2$ was used, with one exception. Also, they used a γ-Al_2O_3 support whereas we used δ-Al_2O_3. Another major difference between these two sets of catalysis is that the catalyst in Desai's work had been chlorinated for 15 min at room temperature whereas our samples had no exposure to Cl_2. The catalyst system studied by Golodov *et al.* (*3–7*) consisted of $CuCl_2$, $PdCl_2$, and LiCl dissolved in water; consequently, the importance of various reaction steps could easily be different. It is perhaps more important to note the similarities that exist in the species present in our model when compared to that of Golodov or Zhizhina.

One difficulty that has existed with the alumina-supported catalysts is the drastic reduction in activity when humidity levels become too high (*1, 2*). This is most likely due to capillary condensation and the filling of small pores in the support, thus decreasing surface area available to the reactant gases. In our use of larger pore δ-Al_2O_3, compared to γ-Al_2O_3 (*1, 2*), we did not observe any reduction in activity, even at humidity levels of 90%, as indicated in Figs. 5d–5e. Even stronger positive dependencies on H_2O were obtained with the more hydrophobic carbon-supported catalysts (Figs. 5h and 5i), thus supporting this explanation. Alumina is hydrophillic and adsorbs water readily whereas carbon is more hydrophobic and interacts much less strongly with water. This behavior can explain not only the different dependence on water pressure as the temperature was raised, but also the negative apparent activation energies. Because of the weaker interaction between water and the carbon surface, a more water-deficient situation occurs at higher temperature, and this leads to an increase in partial pressure dependency on water as the temperature increases. On the alumina-supported catalysts, however, an opposite trend was observed, i.e., a lower partial pressure dependency at higher temperature. Thus, if capillary condensation and pore filling is occurring with the alumina supports, the higher temperatures could actually be increasing the available internal surface area and thereby increasing the rates in this way.

The reason for the negative activation energies observed for all the carbon-supported catalysts in the presence of water vapor can be explained by the weaker bonding of adsorbed water on carbon coupled with the importance of dissolving the Pd and Cu species in a water overlayer on the surface, as stipulated in steps (24)–(26). The reduced water layer coverage at higher temperature provides fewer solvated active species on the surface; consequently, this reduces the activity of carbon-supported catalysts more rapidly than the increase provided by the rate constant. This behavior is well-documented as Fujimoto *et al.* (*26*) reported a negative apparent activation energy for CO oxidation over a $PdCl_2$/carbon catalyst, and Katz and Pismen (*27*) observed a negative apparent activation energy for ethylene oxidation over a carbon-supported Pd Cl_2–$CuCl_2$ catalyst. Although the nearly equal TOFs for the 1.8% Pd–11.9% Cu/C and 0.2% Pd–11.8% Cu/C is an indication of the absence of diffusional limitations, calculations based on the Weisz criterion indicate that the extremely high rates observed with our $PdCl_2$–$CuCl_2$/carbon catalysts in the presence of water vapor are possibly influenced by mass transfer (*28*). This further complicates the analysis of this catalyst system.

Derivation of Reaction Rate Expressions

$PdCl_2$–$CuCl_2$ in aqueous solutions (*5*) is the catalyst commercially using for ethylene oxidation to acetaldehyde in the Wacker process, and the reaction mechanism is relatively well understood for this reaction (*9, 10, 29*). Pd is the only metal that has significant activity in this reaction. Also, CO and ethylene ligands have similar bonding behavior when they interact with transition metals as both have a filled bonding orbital and an unfilled antibonding orbital (*29*). Similarities may therefore exist between the Wacker process and the CO oxidation reaction over $PdCl_2$–$CuCl_2$ catalysts, and the chemistry associated with the Wacker process can provide guidance to that occurring in CO oxidation. For example, our result that the activity ratio of 7.6 between the two Pd–Cu/carbon catalysts is nearly proportional to the Pd loading ratio of 8.3 is in agreement with other studies in which the oxidation rate was linearly dependent on Pd concentration (*30, 31*).

As in the Pd-only catalyst, water plays an important role in CO oxidation, as previously reported by Desai *et al.* (*1, 2*) and Kuznetsova *et al.* (*14*), and the latter authors stated that only water-soluble agents are active in this reaction. The positive effect of water at low temperature was clearly observed in our study as an enormous activity enhancement was found upon the introduction of water vapor. To further confirm this positive effect, the following experiment was performed. The initial activity was measured in the presence of water vapor in the system, then water vapor was removed from the feed and the activity was followed for a certain period of time. Water vapor was reintroduced into the feed and it was determined if the original activity was recovered. This experiment was performed with the 1.8% Pd–11.9% Cu/carbon catalyst at 5.3 Torr water vapor pressure, and the results are shown in Fig. 10. After the H_2O

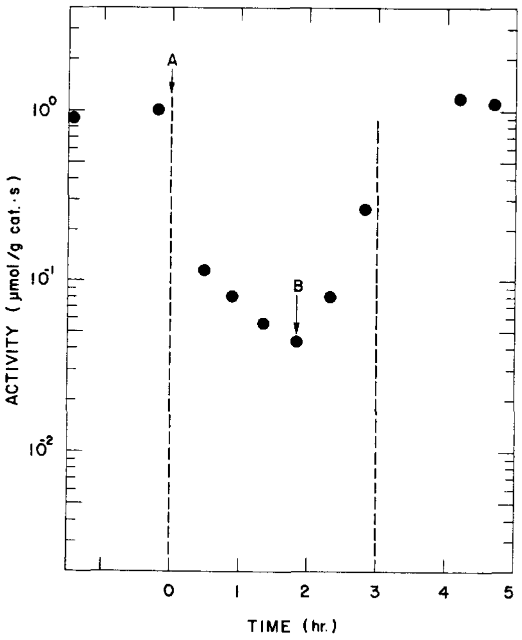

FIG. 10. The influence of water vapor in the feed on activity at 303 K for 1.8% Pd–11.9% Cu/C: Standard conditions; 26 Torr CO, 5.3 Torr H_2O, 132 Torr O_2, balance–He; total pressure = 750 Torr, feed flow rate = 28.5 cm^3/min. (A) Stop water vapor in feed stream. (B) Resume water vapor in feed stream.

vapor feed was stopped, the activity declined substantially over a 2-h period; however, the original activity was fully recovered within an hour by reintroducing water vapor in the feed.

As mentioned in the previous paper (*16*), there is some residual water present on the surface of these supports for partial dissolution and activation of the dispersed metal salts because they were never dried above 373 K. Thus the rate expressions derived from the sequence of steps described in this chapter are based upon a nearly identical set of assumptions:

(1) The most abundant Pd species are PdCl, PdClCO, and $PdClO_2$;

(2) the most abundant Cu species are CuCl, CuClCO, and $CuClO_2$;

(3) an excess chloride concentration exists which is considered to be constant;

(4) when water vapor is present, water can form thin films or islands on the support surface which can solubilize the metal salts and provide a two-dimensional analogue of very active Pd or Cu complexes in homogeneous aqueous systems;

(5) the Pd or Cu complexes in this thin aqueous film are readily accessible to CO and O_2, thus they can be modeled as adsorption sites analogous to those on a solid surface.

For example, Pd and Cu site balances can then be made, i.e.,

$$L_{Pd} = [PdCl] + [PdClCO] + [PdClO_2] \tag{37}$$

$$L_{Cu} = [CuCl] + [CuClCO] + [CuClO_2] \tag{38}$$

where L_{Pd} and L_{Cu} are the total number of Pd and Cu complexes, respectively. The fractions of the metal complexes coordinated with either CO or O_2 for Pd(θ_{CO} or θ_{O_2}) and for Cu(θ'_{CO} or θ'_{O_2}) can be shown to give expressions similar to a Langmuir isotherm, i.e.,

$$\theta_{CO} = \frac{K_{CO}P_{CO}}{1 + K_{CO}P_{CO} + K_{O_2}P_{O_2}}, \tag{39}$$

$$\theta_{O_2} = \frac{K_{O_2}P_{O_2}}{1 + K_{CO}P_{CO} + K_{O_2}P_{O_2}}, \tag{40}$$

$$\theta'_{CO} = \frac{K'_{CO}P_{CO}}{1 + K'_{CO}P_{CO} + K'_{O_2}P_{O_2}}, \tag{41}$$

$$\theta'_{O_2} = \frac{K'_{O_2}P_{O_2}}{1 + K'_{CO}P_{CO} + K'_{O_2}P_{O_2}}, \tag{42}$$

For the Pd–Cu catalysts *without* water vapor in the feed, choosing step (22) as the rds, using the stated assumptions, and employing Eqs. (39)–(42), the rate expression below can be derived (*28*):

$$r = \frac{L_{Pd}L_{Cu}k_3K_2K'_{CO}K_{O_2}P_{CO}P_{O_2}}{(1 + K'_{CO}P_{CO} + K'_{O_2}P_{O_2})(1 + K_{CO}P_{CO} + K_{O_2}P_{O_2})} \tag{43}$$

$$= \frac{kK'_{CO}K_{O_2}P_{CO}P_{O_2}}{(1 + K'_{CO}P_{CO} + K'_{O_2}P_{O_2})(1 + K_{CO}P_{CO} + K_{O_2}P_{O_2})}$$

For the Pd–Cu catalysts *with* water vapor present, using step (35) as the rds and a similar procedure, the following rate expression can be derived (*28*) if water adsorption on the support surface is described by a Langmuir isotherm, i.e.,

$$\theta_{H_2O} = \frac{K_{H_2O}P_{H_2O}}{1 + K_{H_2O}P_{H_2O}},$$

then

$$r = k\left(\frac{K'_{CO}P_{CO}}{(1 + K'_{CO}P_{CO} + K'_{O_2}P_{O_2})}\right) \times \left(\frac{K_{O_2}P_{O_2}}{(1 + K_{CO}P_{CO} + K_{O_2}P_{O_2})}\right) \times \left(\frac{K_{H_2O}P_{H_2O}}{1 + K_{H_2O}P_{H_2O}}\right)^2 \quad (44)$$

Thus in the presence of water vapor, the concentration of very active solubilized Pd and Cu complexes, that is, the maximum number of active sites, will be proportional to the coverage of the H_2O film, as stated in assumption 4, then L_{Pd} and L_{Cu} are proportional to θ_{H_2O} and this gives the second-order dependence on the water concentration on the surface. The final k in (44), $k = L_{Pd} L_{Cu}k_3K_2$, represents a grouping of constants and concentrations that are assumed to be approximately constant at a given temperature.

Using a direct search simplex method for optimization, the constants k, K_{CO}, K_{O_2}, K'_{CO}, K'_{O_2}, and K_{H_2O} in Eqs. (43) and (44) were determined for these $PdCl_2$–$CuCl_2$ catalysts by fitting these equations to the partial pressure data in Fig. 5. These parameters are listed in Table 4, and the calculated rate dependencies are compared with the data in Fig. 5. As perhaps expected with this many fitting constants, our models describe this complicated system relatively well with either Al_2O_3 or carbon supports at two temperatures. More importantly, constants are physically reasonable as the equilibrium "adsorption" constants related to the formation of the complexes are higher at lower temperature. From these values at two temperatures, enthalpies of complex formation can be determined and the ranges obtained from two different reactor systems are relatively narrow, i.e., for PdClCO: $\Delta H = -8$ to -15 kcal/mole; for $PdClO_2$: $\Delta H = -17$ to -19 kcal/mole; for CuClCO: $\Delta H = -6$ to -16 kcal/mole; and for $CuClO_2$ $\Delta H = -28$ to -37 kcal/mole. A literature value of -13.6 kcal/mole has been reported for PdClCO in methyldichloride (*32*), and a value of -18.1 kcal/mole has been reported for $PdClO_2^{31}$. This is remarkably consistent and provides some support for the reasonableness of these models.

The one exception is the set of values for K_{H_2O} for δ-Al_2O_3, but the complication of capillary condensation and pore filling can account for this, as explained earlier. The more hydrophobic nature of the carbon surface prevents this behavior for the carbon-supported catalysts. It is also reasonable that higher equilibrium constants are obtained for CO complexing with these metals than for O_2. These two models can not only fit these bimetallic catalysts, as shown in Fig. 5, but they can also describe the performance of these two metals on other carbons as well as the catalytic behavior of more complicated, multicomponent commercial catalysts containing $PdCl_2$ and $CuCl_2$ dispersed on alumina (*28*).

SUMMARY

Rates of CO oxidation on unreduced Pd–Cu catalysts are much higher than those of monometallic catalysts, and the activity is further enhanced in the presence of water vapor. Again water gives a positive effect on the activity of unreduced Pd–Cu catalysts. The role of this water in CO oxidation over unreduced Pd–Cu catalyst is twofold: first, water vapor is directly involved in the reaction to produce CO_2, and second, it dissolves Pd or Cu species which facilitates their reaction with O_2 and CO to produce the

TABLE 4

Computed Rate Constants (k, K_{CO}, K_{O_2}, K'_{CO}, K'_{O_2}, and K_{H_2O}) for $PdCl_2$ and $CuCl_2$ Dispersed on Alumina and Carbon Supports

Catalyst	Reaction temp. (K)	Constants					
		k	K_{CO}	K_{O_2}	K'_{CO}	K'_{O_2}	K_{H_2O}
1.8% Pd–11.9% Cu/δ-Al_2O_3 (without H_2O, IR)	353	160	450	30	1.2	2.7	—
1.8% Pd–11.8% Cu/C (without H_2O, reactor)	363	47	190	2.1	43	0.27	—
1.8% Pd–11.9% Cu/δ-Al_2O_3[a]	303	250	440	2.3	1200	3.5	97
(with H_2O, IR)	323	600	200	0.42	620	0.015	1300
1.8% Pd–11.9% Cu/δ-Al_2O_3[a]	303	230	140	0.41	370	0.0054	63
(with H_2O, reactor)	323	820	29	0.056	73	0.00031	240
1.8% Pd–11.8% Cu/C (with H_2O, reactor)	303	69	80	21	30	25	98
2% Pd–11.8% Cu/C[b] (with H_2O, reactor)	303	300	0.0053	52	650	2.3	33

[a] E_{act} and ΔH (kcal/mole) were computed from these constants.

[b] Prepared from $PdCl_2$ and $Cu(NO_3)_2 \cdot 5H_2O$.

catalytically active species, which appear to be PdClCO, CuClCO, and possibly $PdCuCl_2(CO)O_2$.

The trends of CO and O_2 partial pressure dependencies over unreduced Pd–Cu catalyts supported on alumina or carbon are not the same as those found in homogeneous catalytic solutions, but they are similar to those reported for reduced Pd metal catalysts. The reason for this is probably due to the better gas contact provided by the very thin water monolayer on the dispersed catalysts, which allows expressions analogous to a Langmuir isotherm to be used in deriving rate expressions invoking homogeneous, aqueous-phase chemistry. The more hydrophobic properties of carbon were utilized to prepare carbon-supported catalysts that had 5- to 10-fold enhancements in specific activity (TOF) compared to Al_2O_3-supported catalysts.

The chemistry proposed in this study of CO oxidation over Pd–Cu catalysts is different from that in previous studies because:

(1) It proposes a one-electron transfer process with the Pd species rather than a two-electron transfer as proposed in the homogeneous Wacker process;

(2) Pd–Cu complexes are assumed to be formed during the reaction;

(3) the rate determining step is the rupture of the O–O bond in a $[PdCuCl_2(CO)O_2]_{aq}$ complex to give CO_2; and

(4) a Langmuir–Hinshelwood-type kinetic model can be applied.

It is quite clear that the different behavior in the adsorption of water vapor on alumina or carbon produces the different activity for CO oxidation on each catalyst. Because of weaker adsorption of water on a carbon surface, the activity is more sensitive to the temperature over carbon-supported catalysts; consequently, negative apparent activation energies can be obtained and greater water vapor dependencies occur at higher temperatures with these carbon-supported catalysts. The unusual decrease in the water vapor dependence at higher temperatures over alumina-supported catalysts is most likely due to the fact that some of the smaller pores, which were filled by capillary condensation, are opened at higher temperature, thereby increasing the available surface area and the number of active sites.

The IR results showed that Pd(I) carbonyls react rapidly with water vapor to form catalysts. This reduced Pd metal is oxidized to Pd(I) by $CuCl_2$ in a series of redox steps similar, but not identical, to those in the Wacker process. This redox mechanism could also be monitored by IR spectroscopy. Based on literature spectra, the CO band at 2158 cm^{-1} was assigned to the carbonyls in a Pd(II) compound, and this was further supported by the fact that this peak was intensified at the expense of the 1930- and 1990-cm^{-1} peaks as O_2 was added into the system. The peak at 1930 cm^{-1} was assigned to the carbonyl in a Pd(I) compound–$(PdClCO)_n$. The 1990-cm^{-1} peak can also be assigned to this species; however, a small contribution from bridged carbonyls on metallic Pd particles cannot be completely discounted. The PdClCO and CuClCO species were clearly identified by IR spectroscopy and they appear to be important catalytically. Reaction sequences involving them which are based strongly on results and proposals in the literature provided rate expressions capable of explaining both the IR and the kinetic results in the presence and absence of water. The rate expressions for these model systems also describe the behavior of more complex, multicomponent commercial catalysts containing $PdCl_2$ and $CuCl_2$.

REFERENCES

1. Desai, M. N., Butt, J. B., and Dranoff, J. S., *J. Catal.* **79,** 95 (1983).
2. Desai, M. N., Ph.D. thesis, Northwestern University, 1980.
3. Golodov, V. A., Kuksenko, E. L., and Sokol'skii, D. V., *Dokl. Akad. Nauk.* **272,** 628 (1983).
4. Kuksenko, E. L., and Golodov, V. A., *Zh. Prikl. Khim.* **61,** 1968 (1988).
5. Golodov, V. A., Kuksenko, E. L., and Taneeva, G. V., *Kinet. Katal.* **23,** 248 (1982).
6. Sheludyakov, Yu. L., and Golodov, V. A., *J. Mol. Catal.* **7,** 383 (1980).
7. Golodov, V. A., and Kyksenko, E. L., *C_1 Mol. Chem.* **1,** 109 (1984).
8. Collins, M. F., *in* "Ventilation '85" (H. D. Goodfellow, Ed.). Elsevier, Amsterdam (1986).
9. Moiseev, I. I., Levanda, O. G., and Vargaftik, M. N., *J. Amer. Chem. Soc.* **96,** 1003 (1974).
10. Vargaftik, M. N., Stromnova, T. A., and Moiseev, I. I., *Russ. J. Inorg. Chem.* **25,** 127 (1980).
11. Zhizhina, E. G., Kuznetsova, L. I., and Matveev, K. I., *Kinet. Katal.* **29,** 130 (1988).
12. Zhizhina, E. G., Kuznetsova, L. I., and Matveev, K. I., *React. Kinet. Catal. Lett.* **31,** 113 (1986).
13. Zhizhina, E. G., Matveev, K. I., and Kuznetsova, L. I., *Kinet. Katal.* **26,** 461 (1985).
14. Kuznetsova, L. I., Zhizhina, E. G., and Matveev, K. I., "Homogeneous and Heterogeneous Catalysts" p. 259. VNU Science Press (1986).
15. Palmer, M. B., and Vannice, M. A., *J. Chem. Technol. Biotech.* **30,** 205 (1986).
16. Choi, K. I., and Vannice, M. A., *J. Catal.* **127** 465 (1991).
17. Goggin, P. L., and Mink, J., *J. Chem. Soc. Dalton* **534** (1974).
18. Dontsova, E. I., *Zh. Prikl. Khim.* **15,** 447 (1942).
19. Byerley, J. J., and Lee, J. Y. H., *Canad. J. Chem.* **45,** 3025 (1967).
20. Sun, K. S., and Cheng, C. H., *J. Amer. Chem. Soc.* **110,** 6745 (1988).
21. Sun, K. S., and Cheng, C. H., *J. Chem. Soc. Chem. Commun.* 209 (1988).
22. Fronczek, F., Schaefer, W. P., and Marsh, R. E., *Acta Crystallogr. Sect. B* **30,** 117 (1974).
23. Vannerberg, N. G., and Brosset, G., *Acta Crystallogr.* **16,** 247 (1963).
24. Heriquez, P., M.S. thesis, Northwestern University, 1976.
25. Zudin, V. N., Likholobov, V. A., and Ermakov, Yu. I., *Kinet. Katal.* **18,** 921 (1977).
26. Fujimoto, K., Iuchi, K., and Kunugi, T., *Int. Chem. Eng.* **12,** 741 (1972).
27. Katz, G., and Pismen, L. M., *Chem. Eng. J.* **18,** 203 (1979).
28. Choi, K. I., Ph.D. thesis, The Pennsylvania State University, 1990.
29. Gates, B. C., Katzer, J. R., and Schuit, G. C. A., "Chemistry of Catalytic Processes," McGraw–Hill, New York, 1979.
30. Ratitskaya, T., Ennan, A., and Paina, V., *Izv. Vyssh. Zaved Khim. Tekhnol.* **21,** 1007 (1978).
31. Valitov, N. Kh., Ibragimov, F. Kh., and Lysikov, V. M., *Kinet. Katal.* **19,** 103 (1978).
32. Dell'Amico, D. B., Calderazzo, F., and Zandona, N., *Inorg. Chem.* **23,** 137 (1984).